THE INCLUSIVE REACTION pp = pX AT THE CERN ISR

P. Strolin and M.G. Albrow

CERN, Geneva, Switzerland

Abstract : Experiments at the CERN ISR have given evidence for proton single-dissociation processes where the missing mass of the system X, measured on the proton which is observed in the reaction $p + p \rightarrow p + X$, presents a distribution extending up to large values, in the 10 GeV range. These processes globally account for ~ 15% of the inelastic p-p cross section. Evidence for such a distinct class of inelastic phenomena is also provided by long-range rapidity correlations and clustering. The nature of these processes appears to be predominantly diffractive. The physics which emerges from ISR observations is discussed, together with a presentation of present and planned lines of experimental investigation at the ISR.

Résumé : Les expériences aux ISR du CERN ont mis en évidence les processus diffractifs dans la réaction $p + p \rightarrow p + X$ pour des masses manquantes allant jusqu'à 10 GeV. Ces processus rendent compte de 15 % de la section inelastique proton-proton. L'évidence pour une classe distincte de phénomènes inélastiques est aussi donnée par les corrélations de rapidité à longue portée et le clustering.

A typical inclusive proton spectrum for the reaction p+p→p+X at PS energies[1] is shown in Fig. 1. As function of the Feynman variable $x = \frac{2p_L}{\sqrt{s}}$, a rather flat continuum is followed above x ~ 0.9 by a structure, which corresponds to the production of resonances in the unobserved channel X. Energy-momentum conservation determines the missing mass to the proton as $M^2 \sim s(1-x)$ to first order. The nature of these processes, where only one of the protons is dissociated, appears to be predominantly diffractive. With increasing s these resonances move towards x=1 and therefore become increasingly difficult to resolve in missing-mass spectra. At ISR energies they are completely smeared out by the experimental x-resolution which at the ISR (c.m. system) is essentially determined by the momentum resolution, measured as the observed width of the elastic peak (elastic events are identified by the presence of a colinear proton in the opposite direction). For instance, at the lowest ISR energy $\sqrt{s}$ = 23 GeV the $N^*(1688)$ bump would occur at x=0.995, whereas the best resolution so far achieved at the ISR is of the order of $\Delta x = \pm 0.006$. At the ISR, proton missing-mass spectra have been measured by the CERN-Holland-Lancaster-Manchester Collaboration and by the Aachen-CERN-Harvard-Genova-Torino Collaboration using magnetic spectrometers equipped with wire chambers.

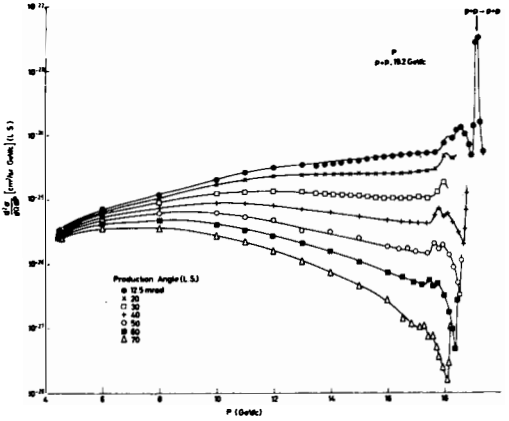

Fig.1. Spectra at fixed angles for the reaction p+p→p+X at PS energies p_{lab} = 19.2 GeV/c. The elastic peak is followed by structure corresponding to the production of resonances.

The dominant, new feature shown by the ISR inelastic proton spectra is (Fig. 2) the presence at x ~ 1 of a peak having a shoulder which extends up to large missing masses, in the 10 GeV range[2)3)]. A valley makes

its appearance between this peak and a broad bump centred around $x \sim 0.5$, which can be interpreted as a leading particle effect (the baryon emerges from the interaction with a substantial fraction of the original energy). The broadening of the inelastic proton peak (although intrinsically much broader than the one which would correspond to the low-mass states identified at PS energies) caused by the experimental missing-mass resolution indicates the experimental problems presented by a detailed study of the missing-mass spectrum at the ISR.

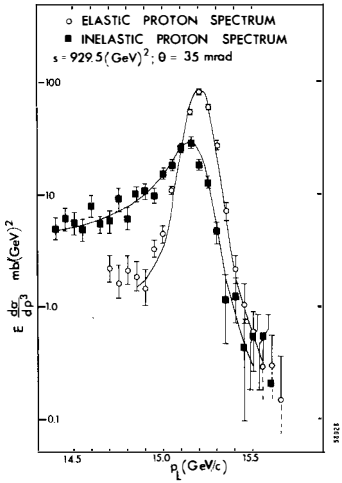

Fig. 2. Spectra for the reaction $p+p \to p+X$ at the ISR, $s = 930$ GeV^2. The elastic peak and the high momentum part of the inelastic spectrum are shown.

Fig. 3 shows in a scatter plot the correlation between the momenta measured by two forward spectrometers situated in opposite arms of an ISR intersection region[3]. The two bands correspond to single-arm

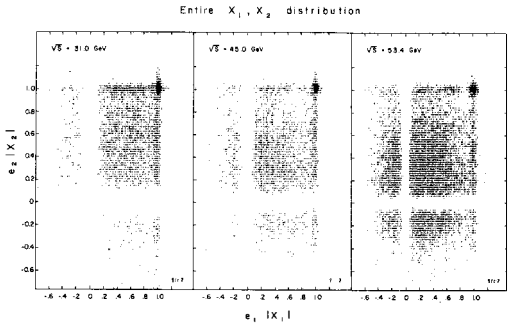

Fig. 3. Distributions of events in e_1x_1, e_2x_2 plane of two particles produced in opposite c.m. hemispheres. $e_i = \pm 1$ is the charge and x_i the scaled momentum of particle i. The elastic peak and the single dissociation bands appear.

dissociation events, in which one observes in one arm a proton(*) having almost entirely kept its momentum and in the opposite arm a fragment resulting from the break-up of the other proton. In the same experiment a number of scintillation counters provided a qualitative indication of the particle multiplicity.

The requirement of no counter hit around the proton at $x \sim 1$ enhances the corresponding band with respect to the rest of the spectrum, indicating the single dissociative nature of the two bands. Moreover, early particle correlation experiments[4] have shown that protons near $x = 1$ are accompanied by particles which tend to be confined within a narrow cone around the colinear direction (Fig. 4a), whereas the requirement of a coincidence with a 90^0 telescope suppresses the inelastic proton peak (Fig. 4b). A positive correlation between missing mass and multiplicity of the break-up particles has also been observed[3] (Fig. 5).

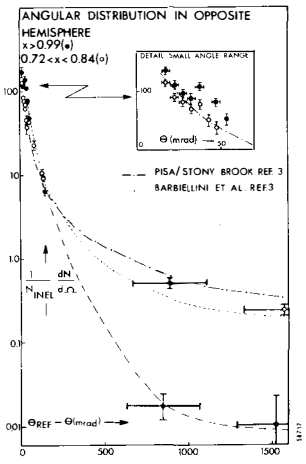

Fig. 4a. Angular distributions of charged particles associated with a proton at $x > 0.99$ and at $0.72 < x < 0.84$.

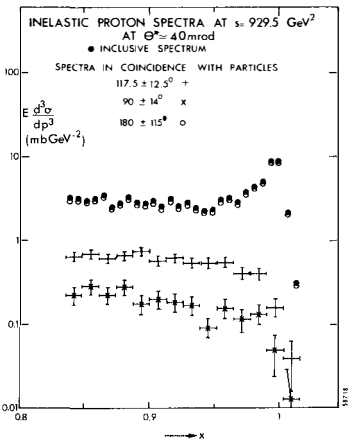

Fig. 4b. Inelastic proton spectra at $\Theta = 40$ mrad with and without the requirement of a coincident charged particle at the angles specified.

*) Positive particle production experiments at the ISR confirm that beyond $x \sim 0.9$ the production of other charged particles is < 1%.

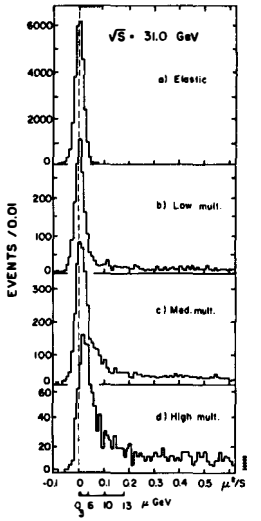

Fig. 5. Missing mass distribution for various crude multiplicity requirements.

A complementary aspect of the process is offered by long-range rapidity correlations. The Pisa-Stony Brook group[5] has measured pseudo-rapidities $\eta = -\ln \tan \Theta/2$ of charged particles produced in inelastic events by means of a 4π counter hodoscope. In the case of single dissociative events, upon discarding the two particles with extreme rapidities (hence also the proton of $x \sim 1$) one is left with a system shifted towards the side of the rapidity plot opposite the proton and characterised by a small dispersion $\Delta\eta$ around its average rapidity $\bar{\eta}$. A two-dimensional histogram $\bar{\eta}$, $\Delta\eta$ of all recorded events shows that for low multiplicities two peaks emerge very neatly as a manifestation of single dissociative events (Fig. 6).

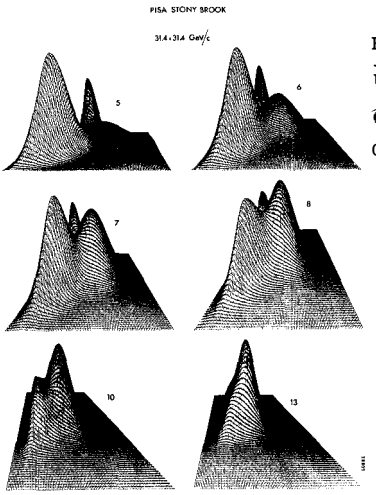

Fig. 6. Two dimensional histograms of $\bar{\eta}$, $\Delta\eta$ for increasing multiplicities of produced particles (Pisa-Stony Brook Collaboration).

Plots at different ISR energies show that these events contribute to larger multiplicities with increasing energy. The rapidity gap between the proton and the rest of the system has recently been used to enhance the single-dissociation signal. A more complete account of these measurements is given by Sanguinetti[5] at this meeting. Kinematic effects should of course be carefully considered in a detailed study.

The interpretation of single diffractive dissociation given to the peak at $x \sim 1$ on the ISR proton spectra clearly involves questions on the dynamical nature of the process. The reference to the low mass states observed at PS energies is, by itself, insufficient for this purpose and on the other hand no exclusive channel has so far been fully analysed at the ISR in order to test quantum number exchanges and assess the presence of absorptive effects which would cause diffraction. The diffractive interpretation must then be based on indirect evidence, such as weak energy dependence, steep t-dependence and large rapidity gaps. We note that a comparison with inclusive n[6] and Λ [7] production, which do not show peaks at $x \sim 1$, already suggests the diffractive (only vacuum quantum numbers exchanged) nature of the inelastic proton peak. Moreover, a peak is observed in pd scattering experiments at NAL, as reported by Olsen at this meeting.

The cross section associated with the single dissociation has been measured both from the missing-mass spectrum measurement (σ_D is of the order of 5 mb at $\sqrt{s}$ = 23 GeV and 31 GeV) and from rapidity distribution (σ_D = 5.8 ± 1, 5.7 ± 1 and 5.8 ± 1 mb at $\sqrt{s}$ = 23, 45 and 53 GeV [5]). Although the errors are still too large to derive the energy dependence of the cross section within the ISR range(*), the process clearly has a cross section comparable both in magnitude and energy dependence to elastic scattering, thus indicating the view that it should be, at least predominantly, related to diffraction.

*) This is specially interesting in relation with the observed rise of the total pp cross section. As discussed by Capella and by Roberts at this meeting, triple-Regge fits of the ISR data, seem to indicate that a good fraction of observed rise of the inelastic cross section could be contributed by inelastic diffraction. Possible improvements of direct measurements of σ_D at the ISR are related to the detection of small momentum transfers, discussed later on in this paper.

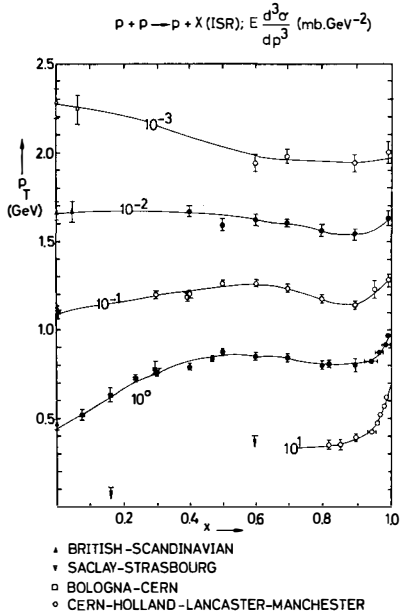

Fig. 7. Contour plot of the invariant cross section for pp→pX at ISR energies in the (p_T,x) plane. Contours are shown at decade intervals of the cross section.

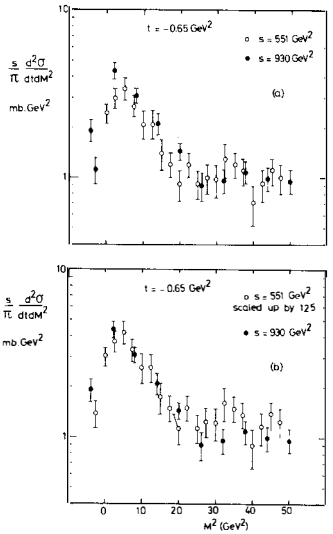

Fig. 8. The invariant cross section at $t=-0.65$ GeV^2 vs M^2 at $s = 551$ GeV^2 and $s = 930$ GeV^2.

The contour plots[8] of constant invariant cross section as function of x, p_T, given in Fig. 7, show that the drop of the differential cross section with transverse momentum is faster for the peak at $x \sim 1$ than for the rest of the spectrum, and therefore support its identification in terms of diffraction. More precisely, the exponential slope of the $x \sim 1$ peak as function of momentum transfer t depends on t and M (the slope is lower for large masses). At the relatively large momentum transfers so far investigated by the ISR missing-mass experiments[2,3], the exponential slope is ~ 5 GeV^{-2}, whereas it is ~ 7 GeV^{-2} at the smaller t-values observed by the Pisa-Stony Brook Collaboration[5]. For comparison, elastic scattering has a slope of the order of 11 GeV^{-2}.

With a minimum angle of ~ 35 mrad, the minimum t observable by the spectrometer of the CHLM Collaboration[2] varies from $-t = 0.17$ GeV at $\sqrt{s} = 22$ GeV to $-t = 1.21$ GeV^2 at $\sqrt{s} = 62$ GeV. The ACHCT spectrometer[3] can observe somewhat, but not substantially, smaller momentum transfers. The s-dependence of the cross section of the peak can therefore be studied only at the lowest energies, owing to the rapid drop of the cross section with momentum transfer. Let us consider the s-dependence in a region where cross sections at the same t, M^2 can be directly compared. Fig. 8 shows the CHLM data[9] at $-t = 0.65$ GeV^2 for $\sqrt{s} = 23$ GeV and $\sqrt{s} = 31$ GeV; the two sets of data agree well in shape, but are higher at the higher s by a factor approximately equal to 1.25. In a simple Regge model the s-dependence at fixed t and M is given by $s^{2\alpha_R(t)-1}$, so that from the above factor one derives $\alpha_R(-t = 0.65) = 0.71$. This value supports the Pomeron as exchanged Reggeon, i.e. indicates a diffractive nature of the process. However, α_R derived in this way is rather sensitive to energy dependent normalization of the cross section and relative to only part of the ISR energy range. Further work, especially running the ISR with 11 GeV in the ring seen by the spectrometer and variable energies in the other ring, will extend these measurements to $t \sim -0.15$ GeV^2 over the range $550 < s < 1480$ GeV^2.

The dependence of the cross section on missing mass at fixed t and s is important for a theoretical interpretation of the data. Within the accuracy of the measurements, a power law of the type $(M^2)^{-B(t)}$, with B certainly function of t (the peak becomes flatter when t increases) agrees well with data. Of course spectrometer resolution has to be unfolded from measured spectra and this certainly represents a delicate problem at the ISR, but the measurement of B is independent of the absolute normalization of the data.

In order to interpret B, in a single Reggeon (i) exchange model, one needs a model for the Reggeon + proton = X vertex. One may use the optical theorem to relate this R-p total cross section to R-p elastic scattering and attempt to describe the latter by a further Regge-exchange amplitude (j). This leads to the well-known triple-Regge diagram, which in the simplest version with no interference terms gives for the invariant cross section

$$\frac{s}{\pi}\left(\frac{d^2\sigma}{dtdM^2}\right)_{iij} \propto G_{iij}(t)\, s^{2\alpha_i(t)-1}(M^2)^{\alpha_j(0)-2\alpha_i(t)} = A(s,t)\,(M^2)^{-B(t)}$$

In this model B does not depend on s, in approximate agreement with experimental data. The terms which are expected to dominate at ISR energy are, at t = 0:

$$\text{PPP} \propto \frac{1}{1-x}$$

$$\text{PPR} \propto \frac{1}{\sqrt{s}}\,\frac{1}{(1-x)^{3/2}}$$

$$\text{RRP} \propto (1-x)^{1-2\alpha_R(0)} \sim \text{constant.}$$

Thus a triple Pomeron coupling (i=j=P with $\alpha_P(0)=1$) would result in a scaling invariant cross section (within ~ 15% in agreement with data, considering the measurement errors and normalization problems) and give B(0)=1.

Fig. 9 gives a compilation of data by the CHLM[9] and ACHGT Collaborations[3]. From the closeness to B(0)=1 of the point at the lowest momentum transfer (B = 0.98 ± .06) the CHLM Collaboration concludes that the triple Pomeron term dominates for $5 < M^2 < 30$ GeV^2, $-t \sim .15$ GeV^2 and $s = 550$ GeV^2. The full trajectory derived from the CHLM data in Fig. 8 is $\alpha_P(t) = 1 + 0.2\,t$. The ACHGT data lie above this line, so that an extrapolation to t=0 of the $\sqrt{s}$ = 31 GeV point, with the above slope

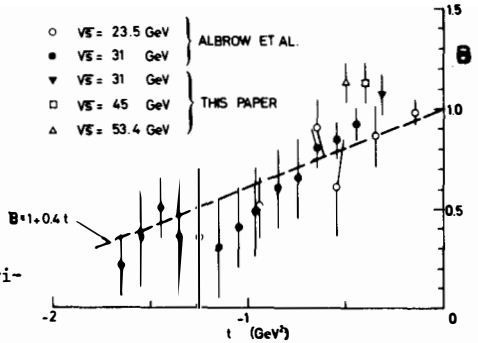

Fig. 9. Fitted values of B(t). The line $B(t) = 1 + 0.4t$, i.e. $\alpha_P(t) = 1 + 0.2\,t$, is straight line fit to CHLM data.

or with a somewhat larger slope (compatible with the CHLM data at the same energy) one obtains $B(0) = 1.2 - 1.3$ which implies an admixture of PPP with PPR. It has however to be noted that because of the poorer resolution the low-mass states $M^2 < 5$ GeV could not be excluded in the ACHGT fits, and on the other hand, that if one would fit the CHLM data with the low-mass points included one would get for B a larger value. More experimental work, especially at small t and with good resolution, is no doubt required.

Fig. 10 shows the rapidity distributions of charged particles observed[10] in association with a proton of given p_L and p_T, and hence the decay distribution in rapidity of clusters with given M^2. The proton has a rapidity $y \sim 3$. As y_{proton} increases the edge of the distribution (y_e) moves rapidly, such that for $M^2 < 18$ GeV^2 essentially all the cluster products are in the opposite hemisphere. For these masses then we observe a large rapidity gap ($\gtrsim 3$ units) which in association with the large single particle cross section is a clear signature of diffraction. The configuration of the events in rapidity space may be represented as in the following schematic diagram. The edge of the cluster is then at $y_e = \ell n\left(\frac{\sqrt{s}}{M^2}\right)$ and the centre at $y_M = \ell n\left(\frac{\sqrt{s}}{M}\right)$. These two points are marked on Fig. 10 and indeed seem to be a good representation of the results.

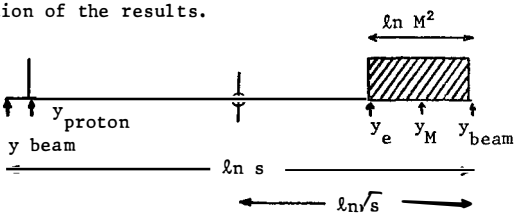

More detailed cluster decay distributions in both Θ and Φ are presently being measured by the CHLM group with a more complete counter system surrounding the intersection.

At NAL the missing mass is measured at very small momentum transfers on the slow recoil proton in the lab system, resulting in a resolution ~ 0.6 GeV^2 on M^2. At the ISR missing mass is measured on the high energy protons scattered at sufficiently large angle to emerge from

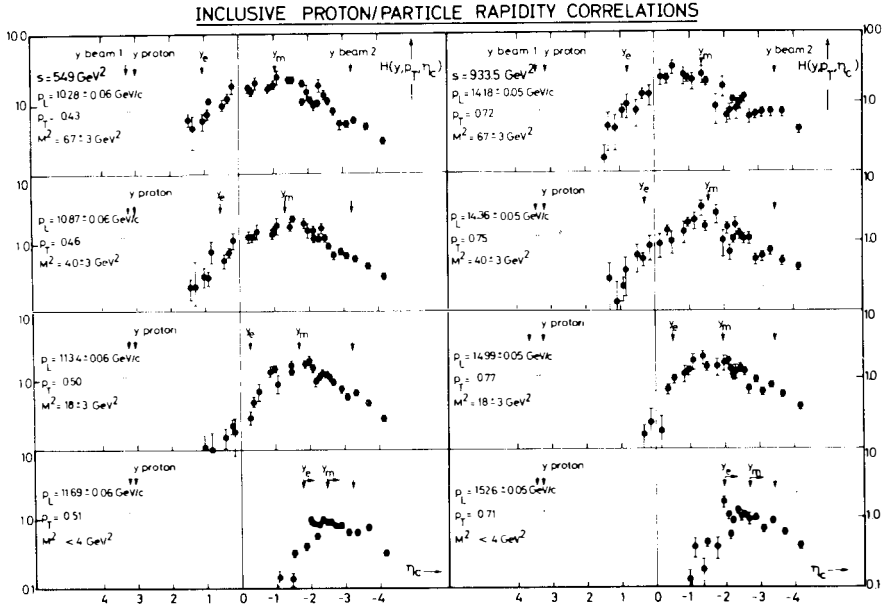

Fig. 10. Distributions in pseudo-rapidity η of charged particles associated with fast protons. For each of two s-values four plots are shown corresponding to various p_L or M_x^2.

the ISR vacuum pipe and enter the spectrometer, so that one obtains a poorer missing-mass resolution and cannot reach very small momentum transfers. No substantial progress is expected for the resolution, other than that resulting from a gradual improvement of the detectors. Measurements at momentum transfers one order of magnitude smaller (i.e. down to $-t = 0.01$ GeV^2) than those so far investigated have been proposed. The instrument required is a mini-spectrometer which detects the small-angle protons at the extreme end of the ISR intersection region as soon as they exit the beam pipe. The use of drift chambers enables one to maintain a momentum resolution of the order of the best so far achieved at the ISR.

Large acceptance spectrometers permit a complete analysis at the system X, with excellent resolution (20 MeV or better) directly from the decay particles. The Aachen-UCLA-CERN Collaboration at the ISR has

collected data using a wire-chamber magnetic spectrometer which has an angular acceptance at ~0.1 rad around the forward direction of X. The spectrometer acceptance limits to a few GeV the range of masses which can be investigated. A preliminary analysis of these data shows the presence at a leading effect (i.e. a peak at $x \sim 1$) in the resultant momentum of a "three-prong inclusive" system observed by the spectrometer. The peak is enhanced if one selects those events which have no particles at $\theta > 400$ mrad in either direction, as the sample is relatively enriched with low-mass, low-multiplicity events fully detected by the spectrometer. Δ^{++} production is found to dominate the observed $p\pi^+$ system. In collaboration with the Harvard,Munich and Riverside groups, data were taken with small wire chambers placed opposite the spectrometer, in order to detect the undissociated proton and, by establishing its colinearity with X, to study exclusive processes such as $p + p = p + (p\pi^+\pi^-)$.

REFERENCES

1. J.V. Allaby et al., Nucl.Phys. B52 (1963) 316.
2. M.G. Albrow et al., Nucl.Phys. B54 (1973) 6.
3. A. Böhm et al., to be published in Nuclear Physics B.
4. M.G. Albrow et al., Phys.Letters 44B (1973) 207.
5. G. Sanguinetti, contribution to this Meeting.
6. J. Engler et al., 2nd Int. Conf. on Elementary Particles, paper 398, Aix-en-Provence (1973).
7. G. Charlton et al., Phys.Rev.Letters 30 (1973) 574.
   M. Blumenfeld et al., 2nd Int.Conf.on Elementary Particles, paper 231, Aix-en-Provence (1973).
8. M.G. Albrow et al., to be published in Nuclear Physics B. Dec. 1973.
9. M.G. Albrow et al., to be published in Nuclear Physics B. Sept. 1973.
10. M.G. Albrow et al., submitted to Phys.Letters, May 1974.